Int. J. Heat Mass Transfer. Vol. 27, No. 2, pp. 273–289, 1984
Printed in Great Britain

0017 9310/84 $3.00 + 0.00

DEVELOPING FLOW AND TRANSPORT ABOVE A SUDDENLY HEATED HORIZONTAL SURFACE IN WATER

J. C. MOLLENDORF, HUMAYUN ARIF† and EMMANUEL B. AJINIRAN‡
Mechanical and Aerospace Engineering, State University of New York at Buffalo, Amherst, NY 14260, U.S.A.

(*Received* 6 *December* 1982 *and in revised form* 1 *June* 1983)

Abstract - The results of this experimental investigation are observations and conclusions, determined by transport measurements and flow visualization, regarding the development of convection above an instrumented, horizontal surface (with side walls) in an extensive water ambient subjected to a step in electrical energy generation. The initial mode of heat transfer was concluded to be conduction, since the measured plate surface temperature closely agreed with one-dimensional transient conduction theory. Departures from the theoretical conduction solution were an indication of the onset of convective motion. When the heated layer became sufficiently thick, a wave-like instability was observed, followed by fluid motion, with nearly-spherically-shaped 'heat bubbles' (thermals) rising randomly, increasing in size, with some assuming a mushroom shape and breaking away from the bulk of the heated fluid. Thereafter, both the local and spatially averaged plate surface temperatures were seen to be time dependent. Another observation was the presence of wispy, swaying 'convection columns' which meandered to-and-fro on the surface. The first visual convective instability was seen to precede the departure of the measured surface temperature from the conduction solution. As the low ambient temperature range was approached, the density extremum effect reduced $Nu\ Ra^{-1/3}$ by as much as about 50%. It is concluded that transport above a heated, horizontal surface in an extensive water ambient is inherently time dependent; initially largely because of 'heat bubbles' breaking away from the conduction layer, and later because of the continual movement of 'convection columns'.

NOMENCLATURE

- b generalizing factor for time, $(k_w/c''\alpha_w)\{1+[\sqrt{(k\rho C_p)_s}/\sqrt{(k\rho C_p)_w}]\}$
- c'' thermal capacity of heating element per unit surface area, $\rho C_p d$
- d thickness of heating element
- g acceleration due to gravity
- Gr_x^* local flux Grashof number, $g\beta L^4 q''/kv^2$
- h convective heat transfer coefficient, q''/θ_0
- i electrical current to foil heated surface
- k thermal conductivity
- l length of horizontal surface
- L average length of plate, $(l+w)/2$
- Nu Nusselt number, $h(\tau)L/k = q''L/k\theta_0$
- $\overline{Nu}$ time average Nusselt number
- Pr Prandtl number, $\mu C_p/k$
- q heat dissipated
- q'' heat flux from foil
- r resistivity of Inconel 600 foil
- R density extremum parameter, $(t_m - t_\infty)/(t_* - t_\infty)$
- Ra Rayleigh number, $g\beta L^3(t_0 - t_\infty)/\alpha v^2$
- $\overline{Ra}$ time average Rayleigh number
- Ra_* experimentally determined critical Rayleigh number
- Ra_δ theoretical break-up Rayleigh number
- t temperature
- t_f film temperature
- t_m temperature of maximum density of pure water, taken to be 4°C
- t_0 surface temperature of plate
- $\bar{t}_0$ time average surface temperature of plate
- t_∞ ambient temperature of fluid
- w width of horizontal surface.

Greek symbols

- α thermal diffusivity, $k/\rho C_p$
- β volumetric coefficient of thermal expansion
- δ instantaneous conduction layer thickness
- θ temperature excess, $t - t_i$
- v fluid kinematic viscosity
- ρ density
- τ time.

Subscripts

- s styrofoam insulation under foil heater
- w water
- δ edge of conduction layer
- 0 location of foil heated surface
- * critical condition indicating departure from the conduction solution.

INTRODUCTION

IN SPITE of their importance in both terrestrial and technological processes, there appears to be relatively less known regarding buoyancy induced flows adjacent to horizontal or nearly horizontal surfaces, than for vertical flows. This is perhaps due to the high degree of complexity of such flows. Problems of geophysical interest concern the onset of convective motion in a deep fluid layer due to heating at a lower horizontal boundary. Certain aspects of micrometeorology involve natural convection flows adjacent to nearly horizontal planes surrounded above by an extensive

† Present address: Fluor Engineers Inc., P.O. Box 35000, Houston, TX 77035, U.S.A.
‡ Last known address: 2 Ilupeju Byepass, Ilupeju, P.M.B. 23186, Ileja, Nigeria.

fluid. Similar flows also arise in many other natural circumstances, such as the surface cooling of ponds, and in numerous technological applications, such as the removal of fog from airport runways and the use of land-based heat sources to stimulate rainfall, see Boehm and Alder [1]. Furthermore, phenomena such as temperature overshoot and inherently time-dependent processes are of considerable importance in material and cooling fluid selection for systems which rely on natural convection cooling or heating. Also, with the advent of the nuclear reactor, transient behavior is becoming increasingly important.

The present experimental investigation was undertaken to attempt to more fully understand the details of the intricate physics of such phenomena. In contrast to natural convection heat transfer from vertical surfaces, the horizontal configuration presents more difficulties for theoretical analysis. The main problem is the very complicated flow pattern. It appears, therefore, that there is a need in analysis for experimentally based guidance. It is the intent of this work to at least partially provide such guidance. The primary difference between the present study and many previous ones is that in the present study the side entrainment of fluid near the heated horizontal surface has been prevented by placing vertical walls around the perimeter of the surface. Consequently, there is no boundary layer flow over the surface because of inflow around the edges.

An analysis of flow adjacent to a horizontal boundary was carried out by Stewartson [2] for a semi-infinite surface, that is, a surface with a single leading edge. A sign mistake in the analysis led to an erroneous conclusion regarding the conditions for the existence of a boundary layer flow on such a surface. This was corrected by Gill *et al.* [3], who showed that the only flow that admits a boundary layer solution for simple boundary conditions is the one generated by a heated surface facing upward with a single leading edge or a similar but cooled surface facing downward.

Robinson [4] gave a theoretical analysis of the convective instability of a growing horizontal thermal boundary layer resulting from a sudden increase in the temperature of a lower horizontal boundary. He modelled his system by applying the Stuart–Watson approach to a study of the nonlinear behavior of slowly growing perturbations to a steady basic temperature profile. The flow development suggested agrees well with both his computed and experimental results, and it is felt that this model provides a most useful aid in the understanding of the nonlinear flow development.

The study of Fishenden and Saunders [5] is similar to the present one inasmuch as it considered transport above a heated horizontal surface. The inclusion of side walls, transient effects and density extrema effects in the present study constitute the major differences between their work and that here. They reported heat transfer correlations for square heated plates facing upward and downward. The particulars of the work from which they derived the correlations are, however, not given. The characteristic linear dimension was taken as the average of the side lengths, with temperature differences between surface and distant air up to 1000°F. The following equations were suggested.

For plates facing upward:

laminar region (Ra between 10^5 and 10^8)

$$Nu = 0.54(Ra)^{0.25}; \tag{1}$$

turbulent region (Ra higher than 10^8)

$$Nu = 0.14(Ra)^{0.33}. \tag{2}$$

For plates facing downward:

laminar region until $Ra = 10^{10}$

$$Nu = 0.25(Ra)^{0.25}. \tag{3}$$

Croft [6] made measurements of the temperature profile in the air immediately above a heated plate by an interferometric method and studied the flow patterns visually and photographically by a direct shadow method. Both the visual observations and temperature measurements show the existence of convection similar to that of the cellular convection noted in shallow enclosed layers. This motion was contained in a layer of some 2 cm in extent, both above a surface in an extensive fluid and in enclosed deep layers. The mean temperature profile in this region was found for a range of surface temperatures and the results show that the logarithm of the mean absolute temperature varies as the $-1/2$ power of the height above the heated surface.

Thomas and Townsend [7] made detailed measurements of the temperature field in natural convection above a heated horizontal surface in air, with and without a cooled upper boundary. Using a variety of experimental techniques, they measured the heat transfer, the mean temperature profiles, mean squares of the temperature fluctuations and the auto-correlation functions of the temperature fluctuations. An interesting feature of these measurements is the close correlation between heat transfer from a single surface and heat transfer between parallel plates.

Townsend [8] extended the above work using improved methods of analysis and observed that the fluctuations of temperature, temperature gradient, and rate-of-change of temperature, all show periods of activity, characterized by large-scale fluctuations, alternating with periods of quiescence with comparatively small-scale fluctuations. Both the proportion and frequency of occurrence of the active periods were reported to decrease with increasing distance from the surface and they probably occur when rising columns of hot air pass through the point of observation. It was concluded that the quiescent fluctuations are typical of the turbulent convection far from the surface while the active fluctuations are the manifestation of the convective processes near the rigid boundary.

Husar and Sparrow [9] performed a flow visualization study of the patterns (in plan view, with side entrainment) of free convection flow adjacent to horizontal, heated surfaces using a technique in which the fluid motions were made visible by local changes of color due to changes in the pH value of the water. The

influence of the shape of the surface on the convective flow was investigated and it was found that, for shapes with corners, a basic characteristic of the convective flow was found to be the partitioning of the flow field.

Sparrow *et al.* [10] performed experiments to explore the qualitative and quantitative characteristics of thermals which ascend through the fluid environment above a heated horizontal surface. Using the same electrochemical technique as described in ref. [9], direct observation of the thermals was performed. Measurements were also made of the fluid temperature above an active site of thermal generation. They concluded that these 'mushroom-like' thermals were generated at fixed sites on the surface, their spacing depending on the heating rate. They confirmed the prediction of Howard [11] that the generation of thermals is periodic, and the break-up Rayleigh number of the conduction layer is $Ra_\delta = 1100$.

Patrick and Wragg [12] studied the onset of free convection using an electrochemical system involving the electrodeposition of Cu^{2+} ions. A number of distinctive flow structures in the transient and steady states were observed including periodic instabilities at transitional Rayleigh numbers leading to pulsations in the convective plumes.

Al-Arabi and El-Riedy [13] determined average and local heat transfer rates in air for the range of Ra from 2×10^5 to 10^9. Plates of different shapes (squares, rectangular and circular) were used and 'corner' and 'edge' effects were investigated. They suggested the following dimensionless equations for the laminar and turbulent regions: Laminar heat transfer (Ra from 2×10^5 to 4×10^7) can be represented, to within $\pm 14\%$ of their data, by

$$Nu = 0.70(Ra)^{0.25}. \quad (4)$$

Turbulent heat transfer (Ra higher than 4×10^7) can be represented, to within $\pm 12\%$ of their data, by

$$Nu = 0.155(Ra)^{0.33}. \quad (5)$$

Similar studies for natural convection adjacent to a horizontal surface have also been carried out [1, 14–20].

Very few of the above investigations have included a flow visualization study. Those who have done so, have considered boundary layer flow over the plate [18], used pH indicators to visualize the flow [9, 10], used air as the fluid under consideration [6, 7], applied electrochemical techniques [1, 12], suspended aluminum particles and illuminated them [15], or used an optical system different from the present study. In all of the above investigations there was inflow over the edges.

The present work concerns an experimental study of transient and developed transport in an extensive and quiescent ambient of water subjected to a step in heat flux from a horizontal surface. Measurements of temperature change with time were taken over the ambient temperature range 1.2–21°C which of course includes the density extremum condition. The

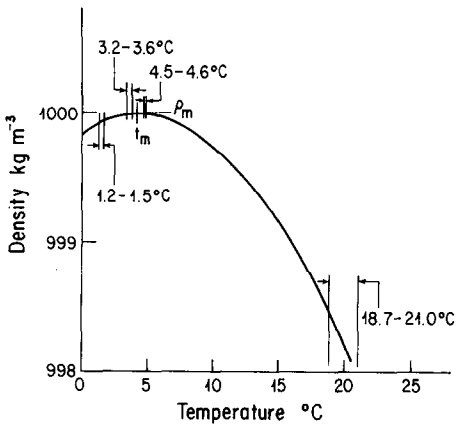

FIG. 1. Heat transfer measurements were taken at the four temperature ranges indicated, whereas flow visualization was done only at room temperature.

following four specific ambient temperature ranges were considered: 18.75–20.9°C, 4.5–4.6°C, 3.2–3.6°C and 1.2–1.5°C, see Fig. 1. For each range, the surface was exposed to a number of heat fluxes. Local and spatially averaged surface temperatures were measured using single thermocouples and a thermopile, respectively. The real-time output was recorded using a digital voltmeter, a strip-chart recorder and an automatic data acquisition system (ADAS). The local and spatial average surface temperature responses were compared with each other and with the following one-dimensional (1-D) transient conduction solution:

$$t_0 - t_\infty = \frac{[q''/k_w b]}{\{1+\sqrt{[(k\rho C_p)_s/(k\rho C_p)_w]}\}} \times \left\{\frac{2}{\sqrt{\pi}}[b\sqrt{(\alpha_w \tau)}] - 1 + e^{\alpha_w b^2 \tau}\,\mathrm{erfc}\,[b\sqrt{(\alpha_w \tau)}]\right\}. \quad (6)$$

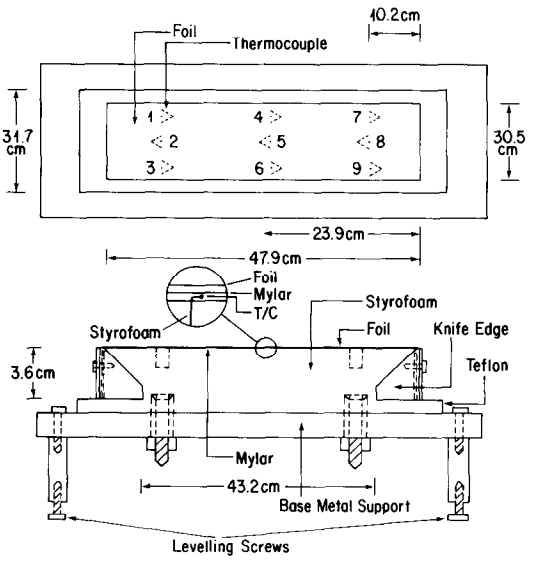

FIG. 2. Heated foil surface and supporting structure (not to scale). Note that side walls (not shown) are abutting the foil heater.

Of particular interest during the transient response was the onset of convective motion and the possibility of temperature overshoot.

EXPERIMENTAL APPARATUS AND PROCEDURE

Heat transfer and temperature measurements

The heated surface consisted of an Inconel 600 foil of dimensions $30.48 \times 47.94 \times 0.00254$ cm thick. The uniformity of the thickness was confirmed using a micrometer. The foil was tightly stretched between two vertical knife edges over styrofoam on a horizontal stainless steel base plate (with adjustable legs for leveling) which was ground flat, see Fig. 2. The styrofoam (4.13 cm thick) was machined flat to a close tolerance and was fitted with nine thermocouples (0.01 cm diameter) bent parallel to the surface and distributed over the entire area. Four thermocouples (2, 3, 6, and 8) were connected to form a thermopile to measure the spatially averaged surface temperature. The local surface temperature was measured with the other thermocouples. Maximum deviation between the readings of the single thermocouples was about 0.1°C when the plate assembly was placed in a constant temperature environment. The thermocouples were electrically insulated from the foil by a layer of mylar (polyfilm ethylene terephthalate) 0.00127 cm thick. For good thermal contact, a very thin layer of silicone grease was applied between the mylar and the styrofoam and between the mylar and the foil. The properties of the composite surface are given in Table 1.

The foil was heated by subjecting it to a step in electrical power by applying a potential difference across the knife-edge terminals. One knife edge was electrically connected to the base metal plate to reduce capacitance effects.

The ratio of the heat transfer from the foil which enters the water, q_w to that which enters the styrofoam backing, q_s, can be estimated from the transient conduction solution (6) given earlier. The result is

$$\frac{q_w}{q_s} \approx \left[\frac{\alpha_s}{\alpha_w}\right]^{1/2}\left[\frac{k_w}{k_s}\right] \approx 47. \qquad (7)$$

Or, the fraction of the total heat to the water is about 98%. All experiments were performed late at night to avoid any large disturbances caused by daytime activity in the building.

The assembly was placed inside an insulated tank of dimensions $76.20 \times 76.20 \times 91.44$ cm high. The tank and the plate surface were levelled, using a precision inclinometer, to within $\pm 1/4°$ from the horizontal. Shock absorption dampers were placed under the supporting legs of the tank to minimize vibrations. The tank was filled with water of high purity to avoid electrolysis and electrical current leakage. Water resistivity of 0.4 MΩ cm was obtained by passing tap water through a reverse osmosis water conditioning system utilizing hollow fibers as the permeable membrane. This water conditioning system rejected not only dissolved materials but also organisms, submicrometer size colloidal materials and bacteria which could contaminate the water. This water was then degassified by passing it through the vacuum chamber of a deaerating apparatus at a pressure of about 1400 Pa. This helped in keeping the water inside the test tank free of bubbles. Five thermocouples were located vertically along the depth of the tank to record stratification.

For heat transfer measurements, the thermocouple response was measured using a Leeds and Northrup Precision Digital Voltmeter having a resolution of 100 nV and an input impedance of 10^{10} Ω up to 16 V. A real-time record of the response was taken with a Beckman Recorder. This instrument has a sensitivity of 5 μV cm^{-1} to 50 V cm^{-1} and high frequency filtering up to 100 Hz. The response time is less than 9 ms for 10–90% of 50 mm.

The water was stirred for about 1 h to equilibrate the temperature throughout the tank. After stirring, a waiting period of about 1 h was necessary to allow all fluid motion to cease. The tank temperature was measured with the five stratification thermocouples, averaged and compared with the reading of a mercury-in-glass thermometer in the middle of the tank. Typical stratification was less than about 0.08°C. At time zero, power was switched over from the auxiliary 'dummy' load to the main heating circuit. A precision shunt resistor of 0.01 Ω and a current rating of 100 A was placed in series with the foil. The current was measured by measuring the voltage across this precision resistor. Power into the plate is then calculated from the voltage and current measurements. Power measurements are estimated to be accurate to within 0.2%.

A four-sided chamber made of vertical, high quality Plexiglas walls, 48 cm high, was placed around the perimeter of the heated surface to prevent inflow and entrainment at the edges and to simulate the condition of ambient fluid extensive only in the upward direction.

Table 1. Properties of materials used in the surface

	Inconel 600	Mylar (ethylene terephthalate)	Styrofoam
k [W m^{-1} K^{-1}]	14.9	0.03751	0.029
ρ [kg m^{-3}]	8415	22.35	35
C_p [J kg^{-1} K^{-1}]	444	1320	1100
α [cm^2 s^{-1}]	0.0387	2.039	0.0075

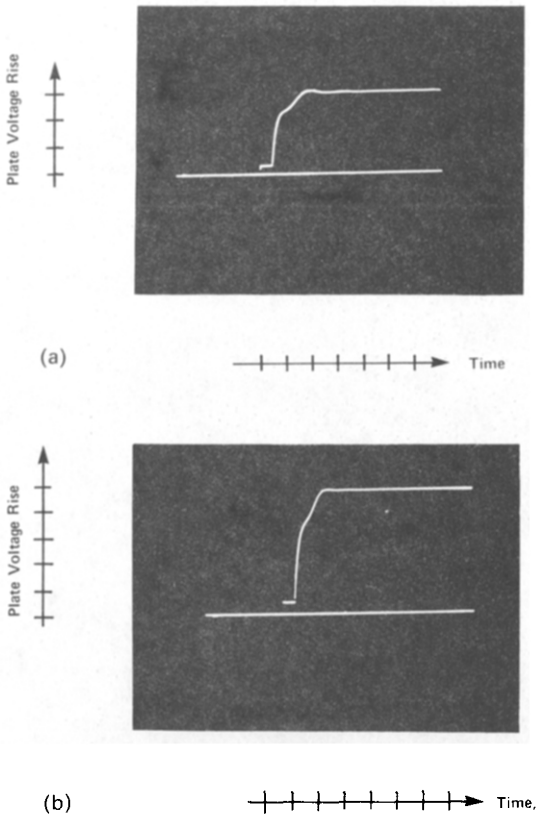

FIG. 3. Transient characteristics of step in electrical power to foil for: (a) $i = 28.64$ A corresponding to about 588 W m^{-2}. Horizontal scale is 50 ms div^{-1}, vertical scale is 1 V div^{-1}. (b) $i = 95.0$ A corresponding to about 5850 W m^{-2}. Horizontal scale is 0.1 s div^{-1}, vertical scale is 2 V div^{-1}.

Two pins 1 cm apart were affixed on the Plexiglas walls to provide a distance scale for the measurements of the size of the instabilities in the Schlieren photographs.

The foil was heated by a step in heat flux created by a step in electrical current from a Hewlett–Packard 6475C DC power supply capable of 0–110 V and 0–110 A. The heating circuit consisted of a primary and secondary one. This was necessary to eliminate transient power surges in the power supply when it was suddenly given a load. A 'slamming' device was employed to switch the connections to the primary circuit. This device was a make-before-break switch which could be operated so swiftly that there is effectively little change in load to the power supply. The quality of the current step was observed by monitoring the voltage drop across the foil on a storage oscilloscope. This response is shown in Figs. 3(a) and (b) for a low and a high current, respectively. It can be seen that the time constant is approximately 200 ms, which is within the specifications of the manufacturer of the power supply and is very fast compared with even the fastest transient studied here.

An overall analysis of experimental errors was done to estimate the maximum errors in: Δt, Nu, Ra, q'', t_∞ and τ. The resulting error estimates are: 1, 2, 3, 0.6, 2 and 3%, respectively.

Flow visualization

A Herschellian arranged Schlieren optical system was used for the flow visualization part of this investigation. This system utilized a 300 W zirconium concentrated arc lamp as a light source, which provided a high intensity yet small source size. Two 30.48 cm diameter high quality, first surface parabolic mirrors with a focal length of 254 cm were used along with a 51 × 61 cm ground glass screen for the image. A horizontal knife-edge permitted vertical gradients to be observed.

For the photographic recording of this investigation, a Nikon F2AS Photomic 35 mm SLR camera was used to photograph the image on the ground glass screen. Winding of the film was facilitated by using a Nikon MD-2 motordrive, and time interval photographs were obtained by using the motordrive with a Nikon MT-1 Intervalometer. The whole camera assembly was fixed on a tripod and the film used was Kodak Tri-X Pan ASA 400. Movies were taken using a Bolex 16 mm movie camera with ASA black and white film pushed to ASA 800. Additional details are given in Ajiniran [21] and Arif [22].

HEAT TRANSFER AND TEMPERATURE MEASUREMENT RESULTS

Seventeen conditions, shown in Table 2, were studied covering a range of heat flux and ambient temperature. It was found in all cases that the initial mode of heat transfer was conduction, since from Figs. 4–7 the surface temperature response is seen to follow the 1-D transient conduction solution (6).

After a 'critical time' depending on the flux level and the tank ambient temperature, a 'critical temperature' was obtained. Figures 4–7 show that at this time, the temperature is seen to suddenly fall below the conduction solution (6) indicating the onset of convective motion. Thereafter the local plate temperature can be seen to oscillate in a somewhat irregular fashion about the steady-state value of the plate.

The local and spatial average plate temperature behaviors are compared in Figs. 6(a) and (b). A single thermocouple was employed to measure the local temperature in Fig. 6(a). A thermopile was used to measure the spatial average plate temperature in Fig. 6(b) for a similar set of conditions. For the single thermocouple, the temperature suddenly fell below the conduction solution at between 180 and 190 s, which corresponds to a temperature difference of about 6.75°C, see Fig. 6(a). The time average temperature was about 5.65°C. The amplitude of oscillation is somewhat lower in the thermopile run probably due to the spatial averaging effect. This comparison suggests that the spatially averaged plate temperature is close to the time average of the local plate temperature. It also suggests that the surface is nearly isothermal, at least during the initial conduction regime.

It can also be seen, from Table 2, that in all runs the critical temperature attained is greater than the time averaged steady-state value. This indicates a certain

Table 2. Conditions and measurements for all heat transfer experiments†

		t_∞(°C)(°F)	q'' (W m^{-2})	t_f(°C)(°F)	θ_0(°C)(°F)	Gr_x	Gr_x^*	$\overline{Nu}$	$\overline{Ra}$	τ_*(s)	θ_*(°F) (°C)	$R=\frac{(t_m-t_\infty)}{(t_*-t_\infty)}$	$\overline{Ra}_*$
18.8–20.9°C	1	19.4(66.9)	709	20.5 (68.95)	2.26 (4.07)	2.48×10^8	4.81×10^{10}	194	0.17×10^{10}	34(L)†	4.82	−6.81	2.01×10^9
										36(U)	2.68		
	2	20.9(69.6)	1140	23.4 (74.02)	4.24 (7.63)	6.94×10^8	9.92×10^{10}	165	0.38×10^{10}	28	8.21	−3.99	4.12×10^9
										32	4.56		
	3	19.4(66.9)	2180	22.1 (71.74)	5.36 (9.65)	6.78×10^8	1.70×10^{11}	251	0.45×10^{10}	18	10.7	−2.87	4.93×10^9
										21	5.93		
	4	18.8(65.7)	2830	22.5 (72.40)	7.39(13.3)	9.69×10^8	2.28×10^{11}	236	0.63×10^{10}	16	13.5	−2.00	6.41×10^9
										18	7.50		
1.2–1.5°C	5	1.2(34.2)	177	3.89(38.99)	5.37 (9.67)	-1.52×10^6	-3.25×10^7	21.3	-1.73×10^7	1700	10.6	0.52	1.90×10^7
										1800	5.90		
	6	1.2(34.2)	369	4.43(39.97)	6.46(11.63)	9.31×10^6	3.45×10^8	37.1	1.04×10^8	650	13.3	0.43	1.18×10^8
										700	7.37		
	7	1.3(34.3)	684	5.40(41.71)	8.19(14.75)	4.20×10^7	2.26×10^9	53.9	4.68×10^8	310	16.88	0.33	5.35×10^8
										320	9.38		
	8	1.2(34.2)	1090	5.97(42.75)	9.54(17.18)	7.13×10^7	5.26×10^9	73.7	7.53×10^8	180	20.14	0.29	8.83×10^8
										190	11.19		
	9	1.3(34.3)	2100	7.77(45.98)	12.9 (23.27)	1.98×10^8	2.06×10^{10}	104	1.97×10^9	85	27.29	0.21	2.31×10^9
										95	15.16		
	10	1.5(34.7)	2690	9.20(48.56)	14.0 (25.20)	3.18×10^8	3.91×10^{10}	123	3.02×10^9	65	30.42	0.18	3.65×10^9
										75	16.90		
3.2–3.6°C	11	3.5(38.3)	684	6.29(43.33)	5.59(10.06)	4.87×10^7	3.83×10^9	78.6	5.09×10^8	180	12.15	0.09	6.15×10^8
										190	6.75		
	12	3.4(38.1)	1130	7.06(44.7)	7.32(13.18)	8.89×10^7	8.75×10^9	98.5	9.05×10^8	110	15.52	0.08	1.07×10^9
										120	8.62		
	13	3.2(37.7)	2180	8.73(47.7)	11.1 (19.92)	2.18×10^8	2.73×10^{10}	126	2.10×10^9	65	22.50	0.07	2.38×10^9
										70	12.50		
	14	3.6(38.5)	656	6.43(43.57)	5.65(10.17)	5.16×10^7	3.84×10^9	74.5	5.38×10^8	180	11.88	0.07	6.28×10^8
										190	6.60		
4.5–4.6°C	15	4.6(40.3)	693	6.91(44.43)	4.61 (8.31)	5.20×10^7	5.00×10^9	96.2	5.33×10^8	130	11.11	−0.13	7.12×10^8
										140	6.17		
	16	4.5(40.1)	1110	7.97(46.35)	6.94(12.49)	1.13×10^8	1.15×10^{10}	102	1.12×10^9	90	13.95	−0.07	1.25×10^9
										95	7.75		
	17	4.5(40.1)	2130	9.82(49.68)	10.6 (19.15)	2.70×10^8	3.44×10^{10}	127	2.52×10^9	55	20.48	−0.05	2.70×10^9
										60	11.38		

† Note that: L = lower bound for critical time; and U = upper bound for critical time.

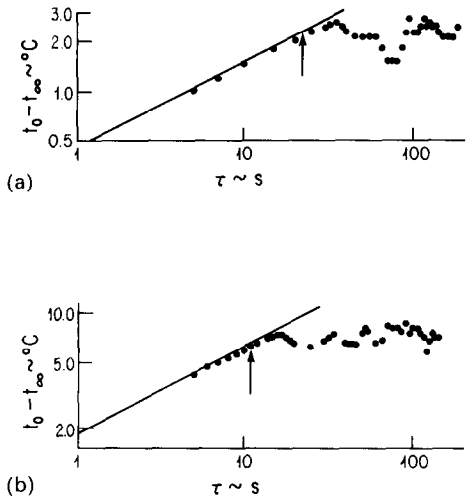

FIG. 4. Comparison of measured average surface temperature with the conduction solution, equation (6), for the 18.8–20.9°C range. (a) Experiment 1, shown in Table 2. Arrow indicates τ_* observed visually, from Table 3, experiment 4. (b) Experiment 4, shown in Table 2. Arrow indicates τ_* observed visually, from Table 3, experiment 2.

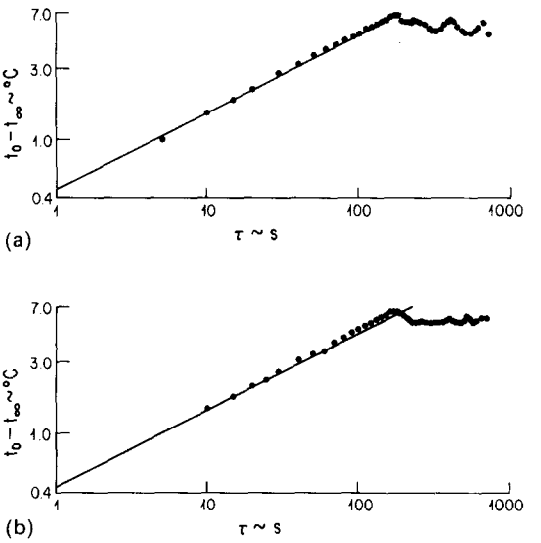

FIG. 6. Comparison of measured average surface temperature with the conduction solution, equation (6), for the 3.2–3.6°C range. (a) Experiment 11, shown in Table 2, single thermocouple. (b) Experiment 14, shown in Table 2, thermopile.

amount of temperature overshoot. It was further observed that the onset of convective motion was highly influenced by both the flux level and the ambient temperature in the tank. The higher the flux level, the earlier motion sets in. This was observed in all runs.

In the low temperature range below t_m, Figs. 5(a) and (b) show delayed transition from conduction to convection. Relatively large surface temperature excursions occurred as the region around the density extremum was traversed during the transient. As the fluid adjacent to the plate surface warms up, its density increases to a maximum at 4°C. Subsequently, it decreases to its initial value and then somewhat below it. Motion then commences.

The density extremum effect on heat transfer was found to increase as the low temperature ambient temperature range was approached. This effect tends to decrease heat transfer. Figure 8 shows that most of our (space and time average) data approximately follow the 1/3 slope of Fishenden and Saunders [5] which they call

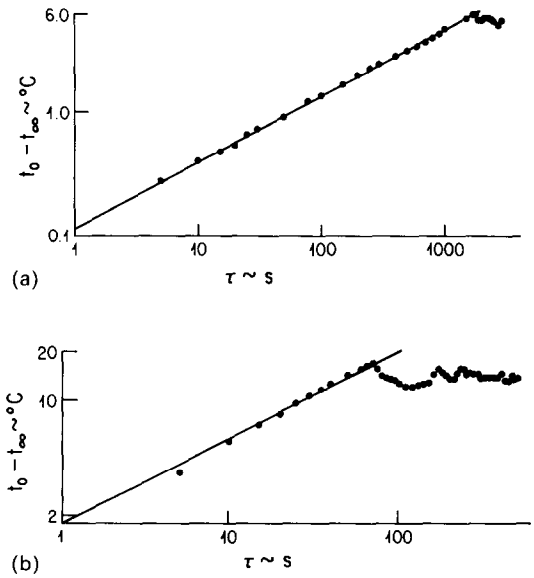

FIG. 5. Comparison of measured average surface temperature with the conduction solution, equation (6), for the 1.2–1.5°C range. (a) Experiment 5, shown in Table 2. (b) Experiment 10, shown in Table 2.

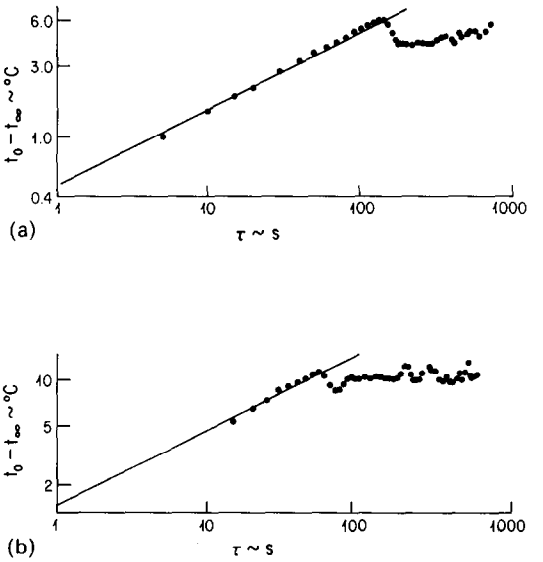

FIG. 7. Comparison of measured average surface temperature with the conduction solution, equation (6), for 4.5–4.6°C range. (a) Experiment 15, shown in Table 2. (b) Experiment 17, shown in Table 2.

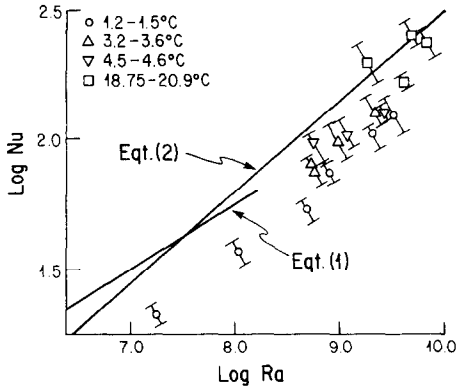

FIG. 8. Comparison of measured average heat transfer with correlations of Fishenden and Saunders [5]. Note that bounding values of each point indicate limits of unsteadiness in average heat transfer and average surface temperature.

the 'turbulent range'. The degree of unsteadiness is shown by the bounds indicated for each data point. Since the higher temperature data is closer to the line, the departure of the low temperature data appears to be due to the effects of the density extremum. Figure 9 shows this more clearly.

The following heat transfer correlation, valid in the vicinity of the density extremum temperature range was obtained

$$Nu\ Ra^{-1/3} = -0.053R + 0.099, \qquad (8)$$

where R is negative for ambients above t_m and positive for those below it. The bounds on data points indicate the limits of the time oscillating values. The RMS error for the fit was found to be about 0.7%. Around the room temperature range, correlation (2) of Fishenden and Saunders [5] was found to be adequate for time and space averaged data, with a corresponding RMS deviation of about 2%. It is clear that for $R > -0.77$ density extrema effects tend to decrease $Nu\ Ra^{-1/3}$.

FLOW VISUALIZATION RESULTS

Some qualitative characteristics of the flow configuration were determined using a Schlieren system. Real-time measurement of the surface temperature variation was simultaneously made to determine the relation between temperature variation and the developing nature of the flow. These measurements were made for four fluxes ranging from 709 to 7867 W m^{-2}. This part of the study was done in water at room temperature, ranging from 19.41 to 21.55°C.

The experimental procedure for flow visualization was essentially the same as for the transport measurements. An HP9825A automatic data acquisition system was programmed to scan all nine thermocouples after a fixed interval of time (3 s in all runs) and record the voltages on a cassette tape for later data analysis. A tenth thermocouple was placed in the ice reference to check the temperature of the ice bath, along with a mercury-in-glass (0.1°C LSD) thermometer. Agreement between the two readings was better than 0.1°C. Forty scans were made of all ten thermocouples in a single run.

A few minutes before each run, the ADAS was programmed to scan the surface thermocouples to check their calibration since at this time they were all essentially at the same temperature. At time $\tau = 0$, the power was switched over to the primary heating circuit. At exactly the same instant, the ADAS and the photographic intervalometer were started.

This investigation resulted in the systematic collection of several hundred photographs showing various stages of convection development for many heat fluxes and different ambient fluid temperatures. It has, therefore, been necessary to restrict the presentation here to selected representative examples shown in Figs. 10(a)–(e) and 11(a)–(e). Photographs of the observed flow field were also compared with the surface temperature measurements in order to observe

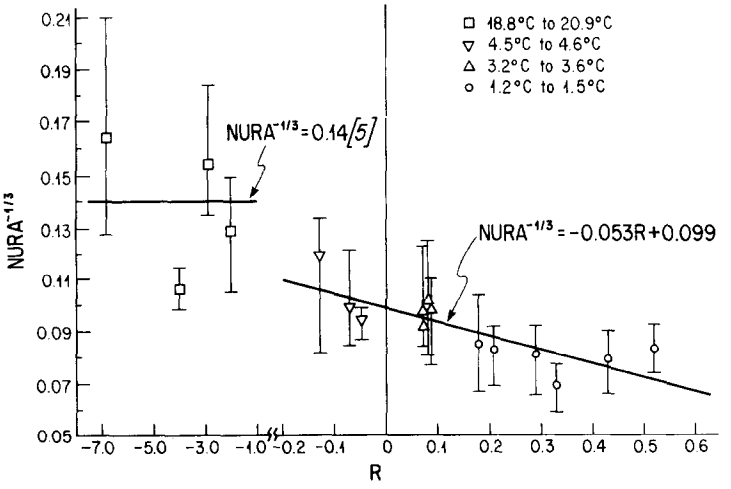

FIG. 9. Departure from Fishenden and Saunders [5] correlation caused by density extremum effects. Note that bounding values of each point indicate limits of unsteadiness in average heat transfer and average surface temperature.

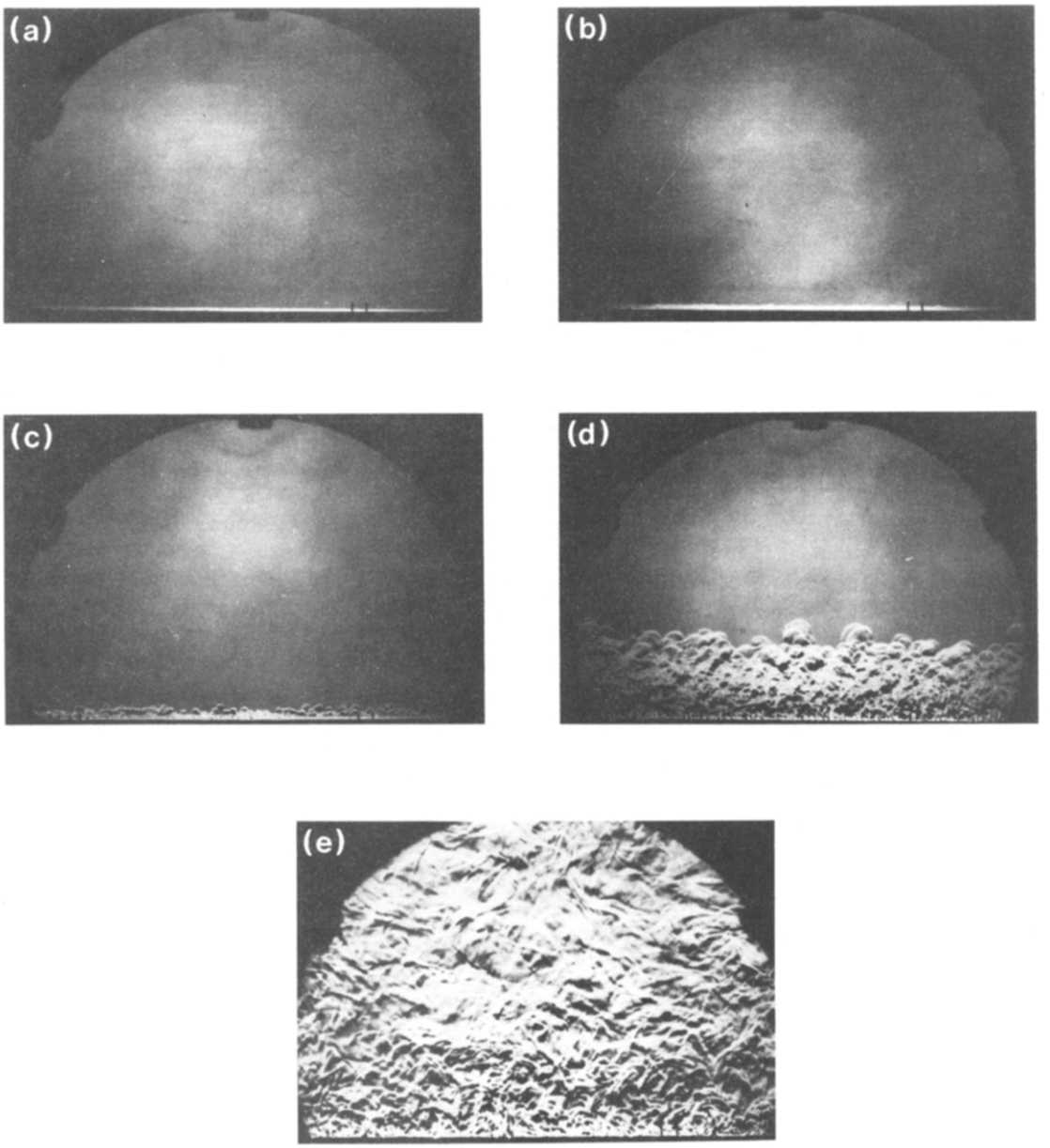

FIG. 10. For $q'' = 7867$ W m^{-2} and $t_\infty = 21.1$°C (run 1, Table 3). (a) Growing conduction layer at $\tau = 4$ s. (b) Onset of convection at $\tau = 6$ s. (c) Generation of laminar plumes at $\tau = 8$ s. (d) Necking of plumes at $\tau = 21$ s. (e) Completely developed flow with convection columns at $\tau = 63$ s.

the relationship between the temperature variation and the flow configuration. The time during the transient of each photograph is indicated. Figures 10(a)–(e) are for $q'' = 7867$ W m^{-2} and $t_\infty = 21$°C, and Figs. 11(a)–(e) are for $q'' = 709$ W m^{-2} and $t_\infty = 21.4$°C.

Figures 10(a) and 11(a) confirm the existence of a growing conduction layer as a horizontal band of heated fluid adjacent to the surface growing in thickness with increasing time. As the conduction layer becomes progressively thicker, an unstable situation arises due to the existence of a less dense layer of fluid (under the heavier bulk fluid) and this leads to instability and the eventual onset of convection, as seen from Figs. 10(b) and 11(b). By comparing the photographs with the surface temperature measurements it is noted that fluid motion is distinctly visible (at about $\tau = 6$ s), before the departure from the conduction solution (at about $\tau = 9.5$ s). See also Figs. 4(a) and (b), where the arrows indicate visually determined departure from a planar conduction layer. This difference suggests that the initial disturbance is not on the surface of the plate, but rather on the outside edge of the conduction layer and it takes time to have its influence felt at the surface. An increase in the heat transfer is then caused by the first main generation of laminar plumes which may be seen to be well established at $\tau = 8$ s in Fig. 10(c). Later, necking of the plumes occurs, at $\tau = 21$ s, Fig. 10(d).

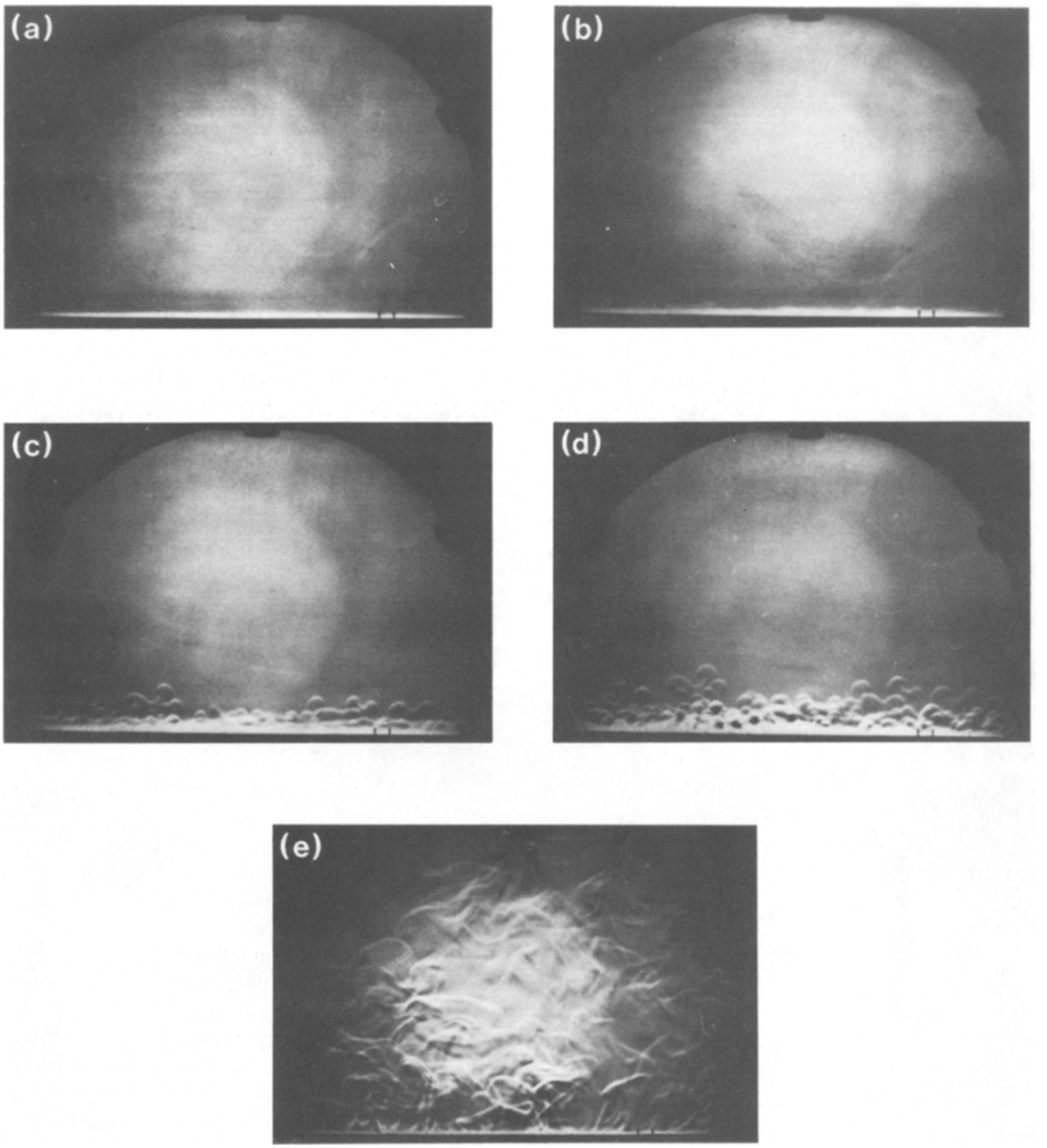

FIG. 11. For $q'' = 709\ \text{W m}^{-2}$ and $t_\infty = 21.4°\text{C}$ (run 4, Table 3). (a) Growing conduction layer at $\tau = 20$ s. (b) Onset of convection at $\tau = 24$ s. (c) Generation of laminar plumes at $\tau = 44$ s. (d) Necking at $\tau = 48$ s. (e) Completely developed flow with convection columns at $\tau = 90$ s.

For sufficiently long times, the onset of convection results in the departure from equation (6) accompanied by a fall in the heat transfer rate and the consequent establishment of 'completely developed flow'. Completely developed flow occurs when convection fills the cavity formed by the side walls, resulting in essentially time invariant time-averaged transport. This is evident from the developed flow seen in Fig. 10(e) ($\tau = 63$ s) in which there is a complex flow structure consisting of a multiplicity of closely spaced interacting 'convection columns' near the surface.

Photographs for the lowest flux studied here are shown in Figs. 11(a)–(e), for the case of $q'' = 709\ \text{W m}^{-2}$ and $t_\infty = 21.4°\text{C}$. Again a marked departure from the conduction solution is noted in Fig. 11(b) with the critical time being much longer, $\tau = 24$ s. Visual observation of the first instability in the conduction layer again precedes the measured time for the first instability in surface temperature. As earlier, the subsequent events leading to developed flow are shown in Figs. 11(b)–(e).

A remarkable difference between the high flux case (Fig. 10) and the low flux case (Fig. 11) is the size of the initial disturbances and subsequent vertical plumes. In the low flux case, the disturbances and the plumes are comparatively larger in size, generated randomly and at

different times, see Fig. 12. With increasing time, these plumes have different rates of ascent (with respect to each other) into the extensive fluid. On the other hand, in the high flux case, the plumes are smaller, generation is much more uniform (that is, initial lift-off instability is over the whole surface) and the rates of ascent (with respect to each other) are also more uniform, so that a 'front' of plumes or thermals seems to be rising, see Fig. 13.

Due to the establishment of developed convection at later times (63–90 s for the four cases) and the limitation of 36 exposures in the film, it was not easy to take enough still photographs over the total flow development time. However, visual observation using a movie [23], showed the formation of a large plume ascending in the middle of the heated surface, being fed by descending fluid from the sides of the central plume. Consequently, two big 'cells' of fluid appear to form on both sides of the central plume. Townsend [8], observed the formation of similar 'cells', but with the direction of the flow opposite to that in the present study. The reason for this difference is perhaps because in the present study no inflow from the sides over the heated surface took place. In the movie it was also observed that several generations of thermals seem to erupt from the heated surface. This process repeated at regular intervals of time, and the eruptions always occur at about the same position on the heated surface, as observed by Sparrow *et al.* [10]. It was difficult to note the time period between eruptions because of the complicated nature of the process and the difficulty of knowing exactly when thermal generation was beginning. A consequence of this unsteady hydrodynamic behavior is that the heat transfer rate never becomes time independent. This is readily confirmed from the oscillatory nature of the transient temperature data shown on Figs. 4–7 after the initial departure from the conduction solution.

DISCUSSION

Flow regimes

It is clear from the photographs that a variety of flow structures exist depending on: (1) the heat flux to the surface and (2) the time during the transient. Three distinct flow regimes are distinguished. In the first regime, close to the heated surface, a growing horizontal conduction layer is present. In the second regime, after the onset of convection and further away from the heated surface, the flow has an orderly multi-plume structure. Finally, in the third regime, still further from the surface, and at later times, the flow is dominated by more chaotic fluid motion.

As soon as the step in heat flux is applied to the surface, warm fluid starts to accumulate slowly at the surface. This is when conduction is dominating. When the conduction layer has persisted for a time slightly less than the critical time, the upper edge of the conduction layer becomes wavy. At critical time, τ_*, the first instability is observed and plume-like structures start developing, rising vertically from the conduction layer. These plumes are a result of small spherically shaped thermals which appear to be related to the waviness of the conduction layer, each thermal breaking off from the crest of a wave. With increasing time, the flow pattern takes on a progressively more multi-columnar form and occurs over all of the heated surface. Then, later, a continuous random generation of convection columns occurs near the surface. As seen from the photographs, the plumes start to neck down as they rise, resulting in mushroom-like appearances at the top, with a hemispherical cap. The thermals were observed to be produced in a periodic process, in accord with the theory of Howard [11]. However, it was difficult to measure the periods between each generation of thermals because it could not be exactly known when a new generation was erupting.

Sparrow *et al.* [10] mention that thermals are generated along a horizontal plane somewhat above the heated surface. The present investigation reveals the persistence of a well-defined layer near the surface even after convection sets in, which agrees with the observation of Sparrow *et al.* [10]. Moreover, in confirmation of their study, the thermals in this experiment were seen to rise vertically as columns of fluid spaced quite regularly along the surface. However, since all visualization here was done from the side, it was difficult to discern the cross-span position of these thermals. Therefore, it cannot be said with certainty that these columns were evenly spaced along the span of the heated surface. Since the thermals could, presumably, be generated anywhere on the surface, the associated columns resulting from these thermals probably do not lie in a single vertical plane. In fact, the pattern observed here is an integrated effect along the total path of the Schlieren light beam.

The thermals are seen to rise generally as a 'front', the spatial frequency and temporal frequency of generation increasing with increasing heat flux. As they go deeper into the ambient fluid, the distance between plumes resulting from the thermals becomes greater. Their upper edges get blunted as they rise, giving a mushroom-like appearance. Some of the larger mushroom caps break away from the bulk of the heated thermals, but this happened very sporadically and only for the highest flux rate.

Once convection had been going on for some time, enough to fill the Schlieren field of view, it was difficult to judge whether thermals were being generated at the same fixed sites because of the completely chaotic nature of the flow field. However, by this time, wispy convection columns had developed, and were seen to parade across the persisting layer near the surface. These convection columns meander to-and-fro on the heated surface. Aiba and Seki [24] suggest that the swaying motion of the convection columns might be a self-excited oscillation related to a periodical variation of local heat transfer on the surface. Since the surface temperature measurements here show unsteadiness, this could explain the motion of the convection

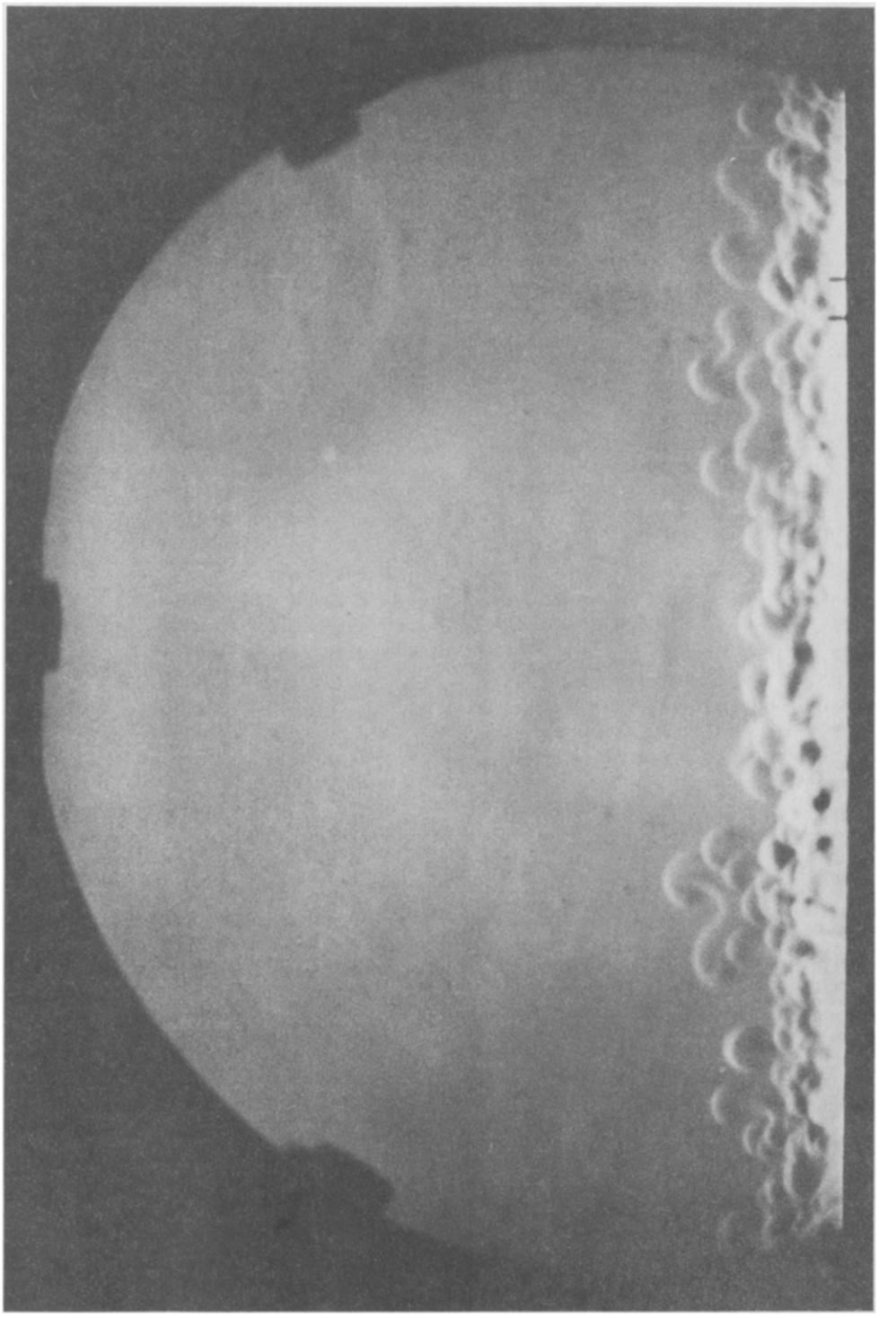

FIG. 12. Enlargement of Fig. 11(d).

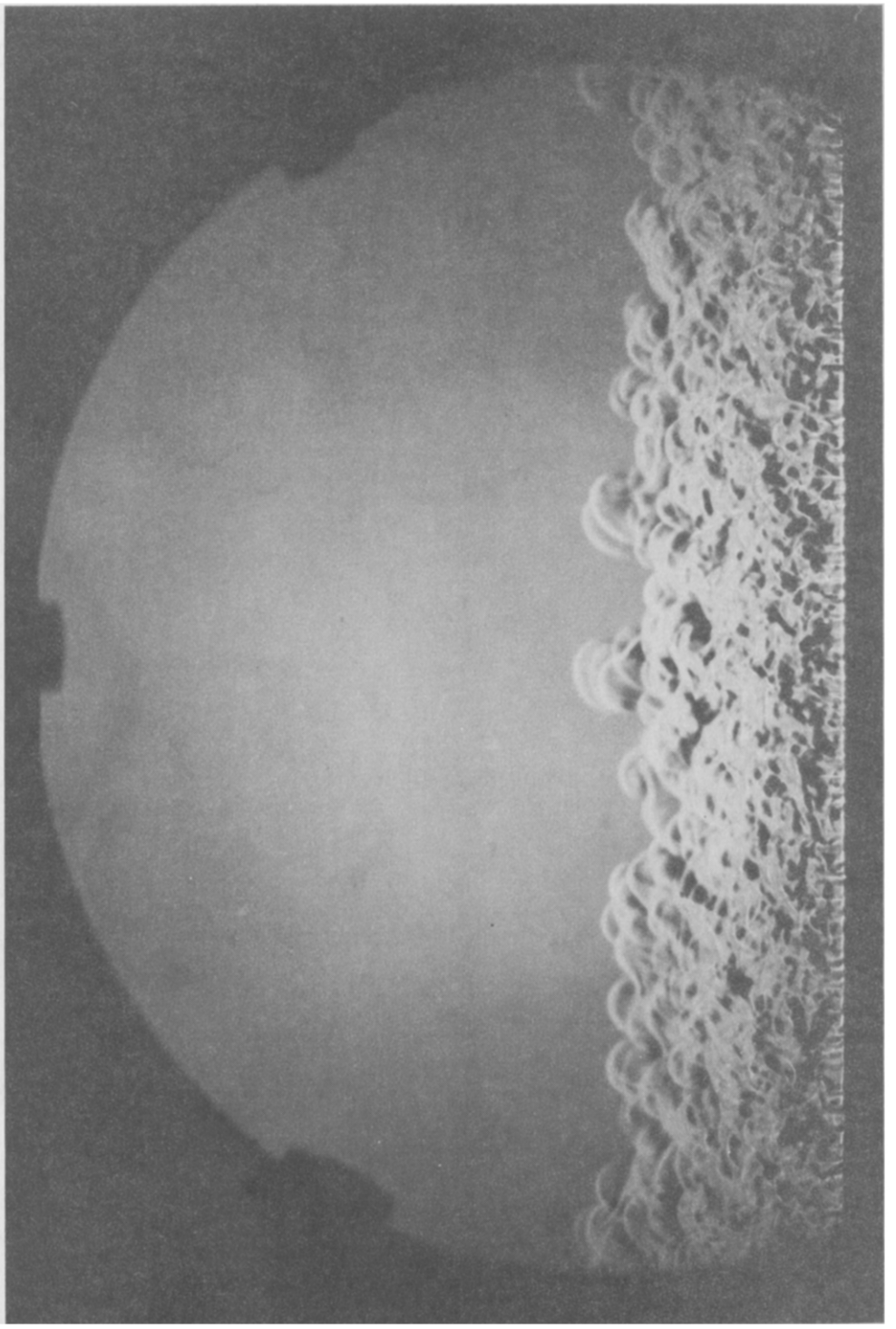

FIG. 13. Enlargement of Fig. 10(d).

columns. Husar and Sparrow [9] also observed the meandering nature of these rising convection columns.

The values of Ra calculated in this experiment are all greater than the transition criteria of $Ra = 10^8$ given by Fishenden and Saunders [5]. Accordingly, from the photographs, all flow regimes in the present investigation are turbulent. However, Fishenden and Saunders [5] apparently did not have side plates to prevent inflow over the edges, as in the present investigation. Therefore, their investigation criteria can not be strictly applied to the present study.

Modes of heat transfer

In all cases, the initial mode of heat transfer is conduction. Visualization of the flow confirmed this by the presence of a conduction layer next to the foil whose penetration depth increased with time until the onset of convection. The variation with temperature of fluid properties such as viscosity and thermal conductivity was unimportant because of the small temperature differences for which each experiment was performed. The influence on the flow configuration due to the heat transfer from the vertical walls which confine the fluid above the heated surface is also expected to be very small, at least for smaller times.

Perhaps the most important observation made in this experiment was the continued persistence of a well-defined layer near the surface even after the onset of convection. The thickness of this layer depended on the heat flux supplied, the depth being smaller with greater fluxes. The persistence of this layer is somewhat different than the phenomenological theory of Howard [11] regarding the generation of thermals, that is: "the convection consists of a mainly conductive phase, $0 < \tau < \tau_*$, during which the conduction layer is built up, followed by a comparatively short interval during which the thermals break off and the layer of warm fluid is swept up in their rising, thus essentially restoring the original conditions, at least near the plate. Another conductive period then ensues, followed by another burst of thermals, and so on". It was observed visually, in the present investigation, that the time required for the thermal to break away from the conduction layer is short compared to τ_* which for moderate and large Pr, agrees with ref. [11]. In all cases, τ_* preceded the measured departure from the conduction solution.

Surface temperature fluctuations

The features of Figs. 4–7 after the departure from the conduction solutions are noteworthy. The temperatures oscillate about an average value. Smaller peaks are also sometimes visible within two bigger peaks. Aiba and Seki [24] investigated this fluctuation and discussed the swaying motion of the convection columns rising from the horizontal plate under the assumption that the motion might be a self-excited oscillation related to a periodical variation of local heat transfer on the surface. According to them, a peak in the temperature fluctuation appeared as a meandering convection column passed over a measuring position, with a small peak as it departs from or approaches there. Another explanation of the surface temperature fluctuations might be the periodic generation of thermals, a peak in the fluctuation coinciding with the generation of thermals.

Critical times

The critical time for the onset of convection is a function of the rate of energy dissipation in the foil and the transport properties of the fluid. In the four flux cases considered, the critical time preceded the departure of measured temperature from the conduction solution. The critical time was observed visually and measured with an electronic timer and also determined by examining the movie film, frame-by-frame, to locate the first time at which an appreciable break-up occurs in the conduction layer. This determination was generally unambiguous to within two frames. In the four runs, the observed critical times varied from 6.2 to 22.5 s.

Critical Rayleigh number

Howard [11] hypothesized that the onset of convection occurs at a specific critical value of the Rayleigh number, Ra_δ (based on the instantaneous thickness of the conduction layer), which can be defined as

$$Ra_\delta = \frac{g\beta[t_0(\tau) - t_\infty]\delta^3}{\alpha\nu}. \tag{8}$$

Several values of Ra_δ have been quoted in the literature: $Ra_\delta = 1100$ (Howard [11]), $Ra_\delta = 2500$ (Elder [25]) and $Ra_\delta = 2800$ (Townsend [8]). In the analysis of Howard [11], δ was taken as $\sqrt{(\pi\alpha\tau_*)}$, where τ_* is the critical time. Values of Ra_δ have been calculated from the present measurements in three ways.

The first is to use values of θ_c and τ_* from Figs. 4–7 (at the point of departure of the measured surface temperature from the conduction trend) and calculate δ using $\delta = \sqrt{(\pi\alpha\tau_*)}$. The resulting average of the Ra_δ values shown in Table 3 is 1778. The second way to infer Ra_δ is to use τ_* from the Schlieren photographs to obtain Ra from Figs. 4–7. The resulting average of the Ra_δ values shown in Table 3 is 943. This lower value reflects the previously noted earlier visually-observed instability, see the arrows on Figs. 4(a) and (b). The third way of inferring Ra_δ is to again use τ_* from the Schlieren photographs to obtain θ_c from Figs. 4–7, but to obtain δ directly from the Schlieren photographs. The resulting average of the Ra_δ values shown in Table 3 is 2584. The first and second ways are expected to be inherently more accurate than the third for two reasons. It is difficult to accurately measure δ directly from the Schlieren photographs because of refraction errors; whereas it is straightforward to accurately measure the critical time, τ_*, at which the first disturbance is seen in a Schlieren photograph. The effect of such an error is compounded because in the first two ways $Ra_\delta \propto \tau_*^{3/2}$; but in the third way, $Ra_\delta \propto \delta^3$. Consequently, the larger expected errors in the values of δ measured from the

Table 3. Conditions and measurements for all flow visualization experiments

Run no.	t_∞ (°C)	q'' (W m^{-2})	$Gr_x^* \times 10^{-10}$	$\overline{Nu}$	$\overline{Ra} \times 10^{-9}$	Second way						First way			Third way	
						τ_* (s)	θ_c (°C)	Ra_δ $[\delta = \sqrt{(\pi\alpha\tau_*)}]$	t_f at τ_* (°C)	Gr_* at $\tau_* \times 10^{-10}$	τ_* (s)	θ_c (°C)	Ra_δ $[\delta = \sqrt{(\pi\alpha\tau_*)}]$	δ (cm)	Ra_δ (δ photo)
1	21.1	7867	3.25	403	13.2	6.2	11	781	26.6	6.68	9.5	14.1	1879	0.29	4190
2	21.5	2840	1.17	344	5.91	11	6.4	1075	24.7	6.42	12.5	6.88	1384	0.30	2617
3	22.0	1772	7.32	278	3.66	12	4.1	784	24.0	4.11	17	4.87	1554	0.32	2034
4	21.4	709	0.29	208	2.10	22.5	2.3	1130	22.6	2.31	33	2.66	2295	0.35	1493

Schlieren photographs are amplified by being raised to the third power.

The values of Ra_δ inferred by the second way are earlier and hence more meaningful indicators of the onset of fluid motion, which appears to begin as a disturbance at the outer edge of the growing conduction layer. Apparently, it takes time for the effect of this disturbance to penetrate to the surface and influence the surface temperature. The large differences between the three average values of Ra_δ (1778, 943 and 2584) suggest that the instability criteria and the method of measurement are important. As explained above, we believe that $Ra_\delta = 943$ (second way) is the most accurate and meaningful indicator of the onset of fluid motion. However, from a heat transfer point of view, $Ra_\delta = 1778$ (first way) has perhaps more meaning.

CONCLUSIONS

Experimental measurements of the surface temperature variation with time, before the critical time (when the heat transfer from a suddenly heated horizontal surface to a one-dimensionally extensive ambient fluid is essentially by conduction) agree well with those predicted by theory. After the onset of convection, the general observations regarding the periodic generation of thermals are in agreement with those of Sparrow *et al.* [10], thereby further validating the qualitative predictions of Howard [11]. However, this periodic generation was clearly observed only in the low flux cases, the flow being too chaotic for clear observation for higher fluxes. Confirmation has also been made of the existence and swaying motion of convective columns near the surface, as did Aiba and Seki [24], under their assumption that the motion might be self-excited oscillations related to the periodical variation of local heat transfer on the surface.

A striking feature of the present observations is the persistence of a quite well-defined layer near the surface even after the onset of convection. Another observed phenomena was that visual observation of the first instability preceded the departure of the measured surface temperature from the conduction solution. This happened in all experimental runs.

After the critical time, the surface temperature is unsteady and fluctuates, characterized by large fluctuations alternating nonregularly with comparatively small ones. It is surmized that a large fluctuation occurs when a meandering convection column of fluid passes through the measuring point (i.e. the thermocouple), while a small one occurs as it departs from or approaches there. Also, the onset of convection and the ensuing flow configuration was highly influenced by the flux level.

It is concluded that transport above a heated, horizontal surface in an extensive water ambient is inherently time dependent; initially largely because of 'heat bubbles' breaking away from the conduction layer, and later because of the continual movement of 'convection columns'.

Acknowledgements—The authors gratefully acknowledge support for this research from the National Science Foundation [ENG7727945], the construction of experimental apparatus by Mr Harold Wagner, and excellent typing by Kay Ward and Elaine Sokolowski.

REFERENCES

1. R. F. Boehm and R. S. Alder, Natural convection arising from stripwise heating on a horizontal surface, *Int. J. Heat Mass Transfer* **16,** 853–855 (1973).
2. K. Stewartson, On the free convection from a horizontal plate, *Z. Angew. Math. Phys.* **9A,** 276–281 (1958).
3. W. N. Gill, D. W. Zeh and E. del Casal, Free convection on horizontal plate *Z. Angew. Math. Phys.* **16,** 539–541 (1965).
4. J. L. Robinson, Theoretical analysis of convective instability of a growing horizontal thermal boundary layer, *Physics Fluids* **19,** 778–791 (1976).
5. M. Fishenden and O. A. Saunders, *An Introduction to Heat Transfer*. Oxford University Press. London (1950).
6. J. F. Croft, The convective regime and temperature distribution above a horizontal heated surface, *Q. Jl R. Met. Soc.* **84,** 418–427 (1958).
7. D. B. Thomas and A. A. Townsend, Turbulent convection over a heated horizontal surface, *J. Fluid Mech.* **2,** 473–492 (1957).
8. A. A. Townsend, Temperature fluctuations over a heated horizontal surface, *J. Fluid Mech.* **5,** 209–241 (1959).
9. R. B. Husar and E. M. Sparrow, Patterns of free convection flow adjacent to horizontal heated surfaces, *Int. J. Heat Mass Transfer* **11,** 1206–1208 (1968).
10. E. M. Sparrow, R. B. Husar and R. J. Goldstein, Observations and other characteristics of thermals, *J. Fluid Mech.* **41,** 793–800 (1970).
11. L. N. Howard, Convection at high Rayleigh number, *Proc. 11th Int. Cong. Appl. Mech.* (edited by H. Gortler). Springer, Berlin (1966).
12. M. A. Patrick and A. A. Wragg, Optical and electrochemical studies of transient free convection mass transfer at horizontal surfaces, *Int. J. Heat Mass Transfer* **18,** 1397–1407 (1975).
13. M. Al-Arabi and M. K. El-Riedy, Natural convection heat transfer from isothermal horizontal plates of different shapes, *Int. J. Heat Mass Transfer* **19,** 1399–1404 (1976).
14. J. V. Clifton and A. J. Chapman, Natural convection on a finite-size horizontal plate, *Int. J. Heat Mass Transfer* **12,** 1573–1584 (1969).
15. T. Fujii and H. Imura, Natural-convection heat transfer from a plate with arbitrary inclination, *Int. J. Heat Mass Transfer* **15,** 755–767 (1972).
16. J. R. Lloyd and W. R. Moran, Natural convection adjacent to horizontal surfaces of various planforms, *J. Heat Transfer* **96,** 443–447 (1974).
17. A. A. Wragg and R. P. Loomba, Free convection flow patterns at horizontal surfaces with ionic mass transfer, *Int. J. Heat Mass Transfer* **13,** 439–442 (1970).
18. Z. Rotem and L. Claassen, Natural convection above unconfined horizontal surfaces, *J. Fluid Mech.* **38,** 173–192 (1969).
19. B. Gebhart, M. S. Bendell and H. Skaukatullah, Buoyancy induced flows adjacent to horizontal surfaces in water near its density extrema, *Int. J. Heat Mass Transfer* **22,** 137–149 (1979).
20. K. Hassan and S. A. Mohamed, Natural convection from isothermal flat surfaces, *Int. J. Heat Mass Transfer* **13,** 1873–1886 (1970).
21. E. B. Ajiniran, Transport from a heated horizontal surface facing upwards in an extensive cold water ambient, M.S. Thesis, SUNYAB (1977).
22. H. Arif, Flow visualization of the development of convection above a suddenly heated horizontal surface in a one-dimensionally extensive ambient fluid, M.S. Thesis, SUNYAB (1981).
23. H. Arif and J. C. Mollendorf, Development of convection above a heated horizontal surface in an extensive fluid, AIChE/ASME 19th National Heat Transfer Conference, Film, Orlando (1980).
24. S. Aiba and N. Seki, A consideration on natural convective swaying motion of plume above a horizontal heated plate, *Int. J. Heat Mass Transfer* **19,** 1075–1076 (1976).
25. J. W. Elder, The unstable thermal interface, *J. Fluid Mech.* **32,** 69–96 (1968).

DEVELOPPEMENT D'ECOULEMENT ET TRANSPORT AU-DESSUS D'UNE SURFACE HORIZONTALE SOUDAINEMENT CHAUFFEE

Résumé—Les résultats de cette étude expérimentale, basés sur des mesures de transport et une visualisation de l'écoulement, concernent le développement de la convection au-dessus d'une surface horizontale instrumentée (avec des parois latérales), soumise à un échelon de chauffage électrique, dans l'eau. Le mode initial de transfert de chaleur est la conduction puisque la température mesurée de la surface s'accorde avec la théorie de la conduction variable unidirectionnelle. Les écarts à la solution théorique de conduction sont une indication du début du mouvement de convection. Quand la couche chauffée devient suffisamment épaisse, on observe une instabilité de type ondulatoire, suivie par un mouvement fluide avec des "bulles de chaleur" (thermiques) de forme sphérique qui s'élèvent au hasard en augmentant de taille, avec une forme de champignon et qui disparaissent au loin. Ensuite les températures locales et moyennes spatiales sur la surface sont dépendantes du temps. Une autre observation est la présence de "colonnes convectives" en touffes qui partent de la surface. La première instabilité convective visible précède l'écart de la température mesurée de la surface à la solution de conduction. Lorsque la température ambiante est faible, l'effet d'extremum de densité réduit $Nu\,Ra^{-1/3}$ d'environ 50%. On conclut que le transport au-dessus d'une surface horizontale chaude, dans une ambiance d'eau de grand volume est foncièrement fonction du temps; initialement à cause des "bulles de chaleur" qui quittent la couche de conduction et ensuite à cause du mouvement incessant des "colonnes convectives".

DAS EINSETZEN VON STRÖMUNGEN ÜBER EINER PLÖTZLICH BEHEIZTEN FLÄCHE IN WASSER

Zusammenfassung—Die Ergebnisse dieser experimentellen Untersuchung bestehen aus Beobachtungen und Schlußfolgerungen über das Einsetzen von freier Konvektion über einer mit Meßfühlern ausgestatteten horizontalen Fläche. Die Fläche (mit seitlichen Begrenzungsflächen) befindet sich in einem ausgedehnten, wassergefüllten Raum und wird sprungartig elektrisch beheizt. Die Ergebnisse wurden durch Messung und Sichtbarmachung der Strömungen gewonnen. Es wurde geschlossen, daß die Wärmeübertragung zuerst durch Leitung stattfindet, da die gemessenen Oberflächentemperaturen der Platte sehr gut mit den nach der Theorie der eindimensionalen instationären Wärmeleitung erwarteten übereinstimmten. Abweichungen von den nach der Theorie der Wärmeleitung erwarteten Lösung sind ein Anzeichen für das Einsetzen von Konvektion. Nach Erreichen einer ausreichenden Schichtdicke wurde eine wellenartige Instabilität beobachtet. Danach setzte eine konvektive Fluidbewegung ein, wobei sich fast kugelförmige "Wärmeblasen" (Thermalen) von der beheizten Oberfläche abhoben und mit fortschreitender Zeit immer größer wurden, wobei einige die Gestalt von Pilzen annahmen und von der aufgeheizten Schicht wegtrieben. Danach waren sowohl die örtlichen als auch die mittleren Plattentemperaturen zeitlich veränderlich. Weiter wurden dünne, hin- und herschwingende "Konvektionssäulen" beobachtet, die auf der Oberfläche hin und her wanderten. Es wurde beobachtet, daß die erste optisch sichtbare Instabilität der Abweichung zwischen der gemessenen und der für Wärmeleitung gerechneten Oberflächentemperatur vorangeht. Bei Annäherung an niedrigere Umgebungstemperaturen verminderte der Einfluß des Dichtemaximums den Wert $Nu\,Ra^{1/3}$ um ungefähr 50%. Zusammenfassend kann gesagt werden, daß der Transport über einer beheizten waagerechten Fläche in einer ausgedehnten Umgebung von Wasser immer zeitabhängig ist: zuerst hauptsächlich wegen der "Wärmeblasen", die sich aus der Schicht mit reiner Wärmeleitung lösen und danach wegen der ständigen Bewegung der "Konvektionssäulen".

РАЗВИТОЕ ТЕЧЕНИЕ И ПЕРЕНОС НАД ВНЕЗАПНО НАГРЕТОЙ ПОГРУЖЕННОЙ В ВОДУ ГОРИЗОНТАЛЬНОЙ ПОВЕРХНОСТЬЮ

Аннотация—Проведены измерения и визуализация потока при возникновении конвекции над снабженной датчиками горизонтальной поверхностью (с боковыми стенками), помещенной в большой объем воды, скачкообразно нагреваемой электрическим током. Предполагается, что в начальный период основным режимом теплопереноса является теплопроводность, так как результаты измерений температуры поверхности пластины хорошо согласуются с теорией одномерной неустановившейся теплопроводности. Отклонения от теоретического решения задачи теплопроводности указывали на возникновение конвективного движения. При достижении нагреваемым слоем определенной толщины наблюдалось возникновение волновой неустойчивости, за которой следовало движение жидкости с почти сферическими "тепловыми пузырьками", которые поднимались беспорядочно, увеличивались в размере, при этом некоторые из них приобретали форму гриба и отрывались от основной массы нагреваемой жидкости. После этого как локальные, так и усредненные по пространству значения температуры поверхности пластины начинали зависеть от времени. Кроме того, наблюдались пучки колеблющихся "конвективных колонок", перемещающихся в обе стороны по поверхности. Отмечено, что первая визуально наблюдаемая конвективная неустойчивость предшествует отклонению измеренной температуры поверхности от значения, полученного при решении задачи теплопроводности. В случае уменьшения температуры окружающей среды влияние экстремума плотности снижало величину $Nu\ Ra^{-1/3}$ примерно на 50%. Сделан вывод, что перенос над нагреваемой горизонтальной поверхностью в большом объеме воды существенно зависит от времени: вначале преимущественно из-за отрыва "тепловых пузырьков", а затем из-за движения "конвективных колонок".